Biomedical Optics EXPRESS

An effective nanosensor for organic molecules based on water-soluble mercaptopropionic acid-capped CdTe nanocrystals with potential application in high-throughput screening and high-resolution optical microscopy

Pick-Chung Lau,[1,*] Robert A. Norwood,[1] Masud Mansuripur,[1] and Nasser Peyghambarian[1]

[1]*College of Optical Sciences, University of Arizona, 1630 East University Boulevard, Tucson, Arizona 85721, USA*
**pickchung@gmail.com*

Abstract: Specially-treated glass substrates coated with a thin film of water soluble mercaptopropionic acid (MPA) capped CdTe nanocrystals (NCs) were prepared and found to undergo photoluminescence changes by as much as 40% when micro-droplets of organic molecules were placed in the nanometer-range proximity of the NCs. This imaging technique involving close proximity between a nano-crystal and an organic molecule is found to provide a 2 × –3 × enhanced contrast ratio over the conventional method of fluorescence imaging. Photoluminescence of NCs is recoverable upon removal of the organic molecules, therefore validating these NCs as potential all-optical organic molecular nanosensors. Upon optimization and with proper instrumentation, these nano-crystals could eventually serve as point-detectors for purposes of super-resolution optical microscopy. No solvents are required for the proposed sensing mechanism since all solutions were dried under argon flow. Fluorophores and fluorescent proteins were investigated, including fluorescein, Rhodamine 6G, and green fluorescent protein (GFP). Furthermore, NC photoluminescence changes were systematically quantified as a function of the solution pH and of the organic molecule concentration. Long duration (> 40 minutes) continuous excitation studies were conducted in order to evaluate the reliability of the proposed sensing scheme.

OCIS codes: (180.2520) Fluorescence microscopy; (160.4236) Nanomaterials.

References and links

1. R. Elghanian, J. J. Storhoff, R. C. Mucic, R. L. Letsinger, and C. A. Mirkin, "Selective colorimetric detection of polynucleotides based on the distance-dependent optical properties of gold nanoparticles," Science **277**(5329), 1078–1081 (1997).
2. A. R. Clapp, I. L. Medintz, J. M. Mauro, B. R. Fisher, M. G. Bawendi, and H. Mattoussi, "Fluorescence resonance energy transfer between quantum dot donors and dye-labeled protein acceptors," J. Am. Chem. Soc. **126**(1), 301–310 (2004).
3. Y. Nagasaki, T. Ishii, Y. Sunaga, Y. Watanabe, H. Otsuka, and K. Kataoka, "Novel molecular recognition via fluorescent resonance energy transfer using a biotin-PEG/polyamine stabilized CdS quantum dot," Langmuir **20**(15), 6396–6400 (2004).
4. K. Aslan, J. R. Lakowicz, and C. D. Geddes, "Nanogold plasmon resonance-based glucose sensing. 2. Wavelength-ratiometric resonance light scattering," Anal. Chem. **77**(7), 2007–2014 (2005).
5. K. Aslan, C. C. Luhrs, and V. H. Pérez-Luna, "Controlled and Reversible Aggregation of Biotinylated Gold Nanoparticles with Streptavidin," J. Phys. Chem. B **108**(40), 15631–15639 (2004).
6. A. J. Haes and R. P. Van Duyne, "A nanoscale optical biosensor: sensitivity and selectivity of an approach based on the localized surface plasmon resonance spectroscopy of triangular silver nanoparticles," J. Am. Chem. Soc. **124**(35), 10596–10604 (2002).

#201235 - $15.00 USD Received 11 Apr 2014; revised 14 Jun 2014; accepted 14 Jun 2014; published 24 Jun 2014

7. D. Roll, J. Malicka, I. Gryczynski, Z. Gryczynski, and J. R. Lakowicz, "Metallic colloid wavelength-ratiometric scattering sensors," Anal. Chem. **75**(14), 3440–3445 (2003).
8. N. Guillot and M. L. de la Chapelle, "Lithographied nanostructures as nanosensors," J. Nanophotonics **6**(1), 064506 (2012).
9. W. C. Chan and S. Nie, "Quantum Dot Bioconjugates for Ultrasensitive Nonisotopic Detection," Science **281**(5385), 2016–2018 (1998).
10. J. Wang, "Biomolecule-functionalized nanowires: from nanosensors to nanocarriers," ChemPhysChem **10**(11), 1748–1755 (2009).
11. N. I. Chalmers, R. J. Palmer, Jr., L. Du-Thumm, R. Sullivan, W. Shi, and P. E. Kolenbrander, "Use of quantum dot luminescent probes to achieve single-cell resolution of human oral bacteria in biofilms," Appl. Environ. Microbiol. **73**(2), 630–636 (2007).
12. L. Zou, Z. Gu, N. Zhang, Y. Zhang, Z. Fang, W. Zhu, and X. Zhong, "Ultrafast synthesis of highly luminescent green- to near infrared-emitting CdTe nanocrystals in aqueous phase," J. Mater. Chem. **18**(24), 2807 (2008).
13. H. C. Ko, C. T. Yuan, S. H. Lin, and J. Tang, "Blinking suppression of single quantum dots in agarose gel," Appl. Phys. Lett. **96**(1), 012104 (2010).
14. W. W. Yu, L. Qu, W. Guo, and X. Peng, "Experimental Determination of the Extinction Coefficient of CdTe, CdSe, and CdS Nanocrystals," Chem. Mater. **15**(14), 2854–2860 (2003).
15. J. M. Dixon, M. Taniguchi, and J. S. Lindsey, "PhotochemCAD 2: a refined program with accompanying spectral databases for photochemical calculations," Photochem. Photobiol. **81**(1), 212–213 (2005).
16. H. Du, R.-C. A. Fuh, J. Li, L. A. Corkan, and J. S. Lindsey, "PhotochemCAD: A Computer-Aided Design and Research Tool in Photochemistry," Photochem. Photobiol. **68**(2), 141–142 (1998).
17. E. Oh, M.-Y. Hong, D. Lee, S.-H. Nam, H. C. Yoon, and H.-S. Kim, "Inhibition assay of biomolecules based on fluorescence resonance energy transfer (FRET) between quantum dots and gold nanoparticles," J. Am. Chem. Soc. **127**(10), 3270–3271 (2005).
18. R. Sjöback, J. Nygren, and M. Kubista, "Absorption and fluorescence properties of fluorescein," Spectrochim. Acta, Part A **51**(6), L7–L21 (1995).
19. F. Koberling, A. Mews, and T. Basché, "Oxygen-Induced Blinking of Single CdSe Nanocrystals," Adv. Mater. **13**(9), 672–676 (2001).
20. P. C. Lau, R. A. Norwood, M. Mansuripur, and N. Peyghambarian, "An effective and simple oxygen nanosensor made from MPA-capped water soluble CdTe nanocrystals," Nanotechnology **24**(1), 015501 (2013).
21. W. G. J. H. M. van Sark, P. L. T. M. Frederix, D. J. Van den Heuvel, H. C. Gerritsen, A. A. Bol, J. N. J. van Lingen, C. de Mello Donegá, and A. Meijerink, "Photooxidation and Photobleaching of Single CdSe/ZnS Quantum Dots Probed by Room-Temperature Time-Resolved Spectroscopy," J. Phys. Chem. B **105**(35), 8281–8284 (2001).
22. H. Morise, O. Shimomura, F. H. Johnson, and J. Winant, "Intermolecular energy transfer in the bioluminescent system of Aequorea," Biochemistry **13**(12), 2656–2662 (1974).

1. Introduction

A quantum dot, also known as a nanocrystal (NC), is a semiconductor material in which the electron-hole carriers are confined in all three spatial dimensions. Unlike a typical atom, these NCs have dimensions on the order of 1-10 nm, therefore creating a type of material that bridges the gap between bulk semiconductors and single atoms and molecules. In recent years, NCs have been extensively researched for detection and labeling of biomolecules due to their size dependent fluorescent characteristics. As a result, several optical techniques utilizing NCs have been developed for molecular recognition. These include colorimetric detection [1], fluorescence resonance energy transfer (FRET)/quenching [2,3], surface plasmon resonance analysis [4,5], and scattering based nano-sensing [6–8]. These techniques utilize the biomolecule conjugated NCs to detect biospecific interactions; in particular, they have been successful in FRET based studies due to their distinct optical characteristics [2,3,9].

However, to the best of our knowledge, none of these detection techniques have been applied on a dried NC thin film, immobilized on a chemically functionalized glass substrate. Unlike conventional optical microscopy techniques, these NCs are used as single pixel nanosensors on a 2D glass substrate where their photoluminescence undergoes changes whenever foreign molecules are placed in their nanoscale proximity.

In this paper, we demonstrate a simple and solvent free optical biosensing technique, where photostable water-soluble CdTe NCs undergo reversible photoluminescence (PL) quenching upon close interaction (nanoscale) with fluorophores and fluorescent proteins. Our results show an improved contrast ratio (by a factor of 2-3) using the NC-organic molecule

#201235 - $15.00 USD Received 11 Apr 2014; revised 14 Jun 2014; accepted 14 Jun 2014; published 24 Jun 2014

close proximity (abbreviated as NC-cp) imaging method when compared to the conventional fluorescence imaging technique. The areal density of the fluorophores and fluorescent proteins were maintained within the range of pmol/cm^2, which is an ultralow concentration regime in many applications [10,11]. Such NC thin films as reported in the present paper could provide a simple approach to high throughput and high sensitivity screening for molecular detection and potentially for super-resolution optical microscopy.

2. Procedure

2.1 Chemicals

Cadmium nitrate tetrahydrate, purum > 99.0% (Sigma Aldrich, 20911), tellurium powder, 200 mesh, 99.8% (Sigma Aldrich, 266418), 3-mercaptopropionic acid (MPA) > 99% (Sigma Aldrich, M580-1), sodium borohydride, powder > 98% (Sigma Aldrich 452882), N^1-(3-trimethoxysilylpropyl) diethylenetriamine (APTES) - technical grade (Sigma Aldrich, 413348), hydrogen peroxide, 50 wt% (Sigma Aldrich, 516813), sulfuric acid, 99.999% (Sigma Aldrich, 339741).

2.2 Synthesis of NaHTe precursor solution

Preparation of NaHTe was done based on Zou Lei *et al* [12] for ultrafast precursor synthesis. 50.8 mg of tellurium powder was added to a 100 mL three-neck flask followed by 37.8 mg of sodium borohydride. The flask was then purged with argon gas for at least 5 minutes. Subsequently, 10 mL of argon saturated distilled (DI) water was injected into the flask via a 15 mL syringe. The 3-neck flask was then immersed in an 80°C water bath for 30 minutes.

2.3 Synthesis of CdTe + MPA nanocrystal

This method was a modification of the standard procedure developed by Zou Lei *et al* [12]. In short, 40 mL of argon saturated DI water was inserted into a 100 mL three-neck flask. This was followed by insertion of 0.2 mmol of Cd^{2+} precursor solution (previously prepared by dissolving cadmium nitrate tetrahydrate in DI water). 0.34 mmol of 3-mercaptopropionic acid was then added into the solution. Subsequently, the pH was adjusted to 11.9 by drop-wise addition of NaOH. While stirring, 0.02 mmol of freshly prepared NaHTe was swiftly injected into the solution. The temperature was then gradually increased using an oil bath to 100°C. NCs were grown for 25 minutes. At this point, a total of 0.4 mmol of MPA was added gradually over a period of 10 minutes. CdTe + MPA NCs were then grown for another 45 minutes before samples were taken. The resulting NCs have their peak photoluminescence at 615 nm.

2.4 Sample preparation of CdTe + MPA nanocrystal

VWR vista vision cover slips (0.16-0.19 mm thickness) were used as the glass substrate to which to attach NCs. These cover slips were first piranha-etched (1:3 by volume hydrogen peroxide to sulfuric acid) for 30 minutes. Coverslips were then immersed in 2% 3-aminopropyltriethoxysilane (APTES) solution in ethanol for 1 hr at 70°C. A dilute NC solution (50x dilution that produces a NC coverage of 150 ± 30 NCs per square micron on glass substrate) was later spin coated onto the cover-slip. Cover-slips were subsequently washed with flowing DI water to remove any excess NCs that were weakly attached through ionic interactions. The remaining NCs that were attached to APTES via zwitter-ionic bonds were dried on a 50°C hot-plate.

2.5 Creating micro-droplets on CdTe nanocrystal-coated substrate via tapered glass tube spraying method

Initially a 50 microliter capillary glass tube (VWR 53508-466) is hung on a weight and pulled by applying extreme heat in the middle. As a result, we obtain a sharp tapered glass tube with

#201235 - $15.00 USD Received 11 Apr 2014; revised 14 Jun 2014; accepted 14 Jun 2014; published 24 Jun 2014

an inner diameter of ~15 microns. Organic molecule solutions (volume~1 microliter) enter the tapered glass tube via capillary action. Upon fast injection perpendicular to the surface of the NC-coated substrate, we are able to create a spray of micro-droplets, which is subsequently examined under a fluorescence microscope.

Acquiring good NC-cp images (such as those shown in Fig. 5, for example) requires that the droplets be homogenous and micron-sized. This allows non-affected NCs to fall within the field of view of the image for accurate contrast ratio measurements. So far, the spray method is found to be the only reliable and cost effective method of producing good NC-cp images. No doubt the current spray method can be improved using more accurate positioning and a more reliable injection tool; however, for purposes of the present experiment, the current technique is more than adequate for reliable NC-cp measurements.

2.6 Fluorescence microscope setup

All PL measurements were carried out under a wide-field fluorescence microscope (Zeiss Axio Imager Z2). The NC sample was mounted such that the gas line was placed within 1 mm above the surface with a fixed flow rate of 5 lpm (Fig. 1). The gas line was premixed to the proportion of interest using a digital mass flow controller (Sierra Instrument C101-DD-2, range: 0.2-10 sccm) for the oxygen source and a flow meter (Matheson, range 0.5-25 lpm) for the argon source. The PL of the NCs was collected by an oil immersion 100X objective lens (NA = 1.45) and detected by an air-cooled EMCCD camera (Photonmax 512B) after passing through an emission bandpass filter at 605 ± 15 nm. The exposure time was fixed at 2 seconds. The camera background values were measured and accounted for in all PL measurements. A mercury arc lamp (HBO 100) was used as the source, and the excitation wavelength was fixed at 405 nm with FWHM of 50 nm. The maximum irradiance was measured at around 12 W/cm^2.

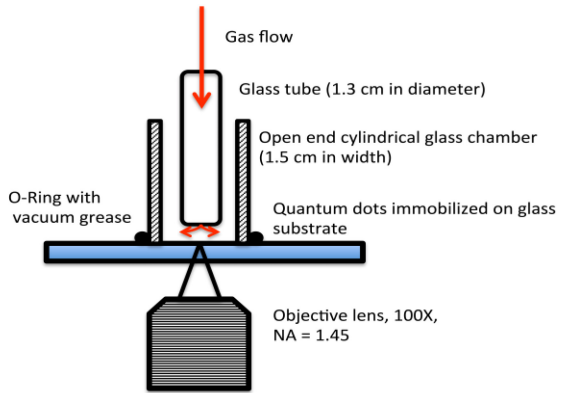

Fig. 1. System setup for measuring the PL of CdTe NCs as well as that of dye molecules under argon gas flow. The illumination is through the bottom of the glass substrate, The PL signal was collected in the reflected path toward the EMCCD, also from the bottom side of the substrate.

2.7 CdTe + MPA nanocrystal photoluminescence and absorption measurement

The PL spectrum of CdTe + MPA NCs in deionized (DI) water was acquired using the Quanta Master 40 steady state fluorescence spectrofluorometer from Photon Technology International (PTI). Excitation wavelength was fixed at 405 nm with 500 ms exposure time and 1 nm slit size for both excitation and emission acquisition. A Cary 300 UV-Vis spectrophotometer is used to measure the absorption spectrum.

#201235 - $15.00 USD Received 11 Apr 2014; revised 14 Jun 2014; accepted 14 Jun 2014; published 24 Jun 2014

2.8 TEM measurement

All NCs were measured using the Hitachi-8100 TEM. The samples were placed on an ultrathin carbon film on a 400 mesh copper grid (Ted Pella-01822).

3. Results

3.1 CdTe + MPA NCs have extreme photostability and can be immobilized using APTES functionalized glass substrates

We use a simple method to systematically quantify the proximity interactions of NCs with fluorophores and fluorescent proteins. The strategy involves adding micro-droplets of organic dyes to a thin layer of NCs coated on a glass substrate. However, there are some conditions to be met: (1) NCs must not photobleach; and (2) NCs must be anchored on the glass substrate such that they do not drift away after addition of micro-droplets. Issue (1) is resolved by purging NCs with argon gas. It is found that MPA-capped water-soluble CdTe NCs are highly stable in an argon environment and do not exhibit any signs of photobleaching over time [13]. Issue (2) is addressed by immobilizing NCs on a 3-aminopropyltriethoxysilane (APTES) functionalized glass substrate. After rinsing with ethanol and/or water, NCs do not exhibit any signs of coming off or photo-degradation (Fig. 2).

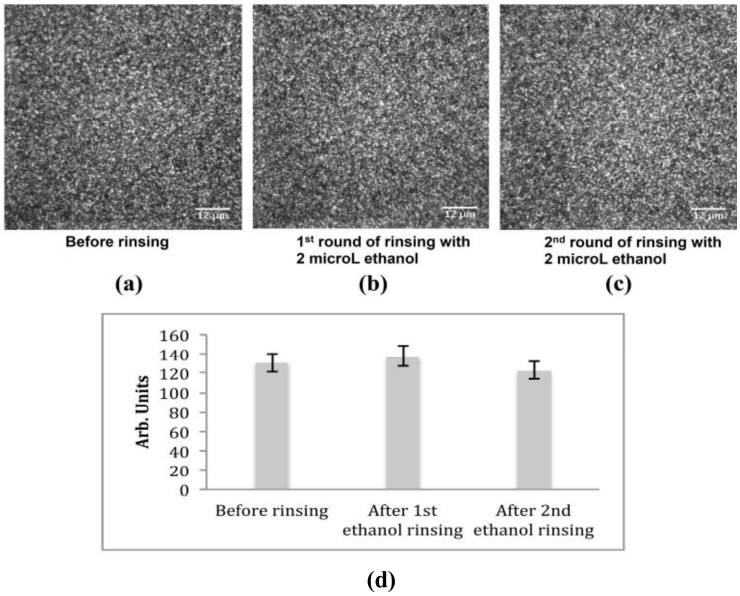

Fig. 2. Photoluminescence of NCs as collected by an EMCCD camera (described in procedure) with a fixed exposure time of 500 ms. The emission filter was set at $\lambda = 605 \pm 15$ nm, coinciding with the peak emission of the NCs. (a) PL profile of water soluble MPA capped CdTe NCs before rinsing. (b) PL profile of NCs after 1st round of ethanol rinsing. (c) PL profile of NCs after 2nd round of ethanol rinsing. (d) Averaged PL count per pixel (after background subtraction) for each case (a)-(c). Upon rinsing with ethanol, no significant PL decay or removal of NCs was detected. Similar results were obtained for NCs rinsed with water.

Two sizes of NCs (peak emission at 615 nm and 655 nm) were used in later experiments. The smaller NC particles have an average diameter of 3.45 nm with RMSE of 15%. No TEM measurements were conducted on the larger NCs; however, an estimate based on Yu et al [14] shows that the diameter is approximately 3.91 nm. In order to minimize the spectral crosstalk, the smaller NCs (abbreviated as NC 615) were used to observe the presence of fluorescein, while the larger NCs (abbreviated as NC 655) were tailored for detecting Rhodamine 6G. Different spectral pass-bands were used, as shown in Fig. 3, for optimal detection.

#201235 - $15.00 USD Received 11 Apr 2014; revised 14 Jun 2014; accepted 14 Jun 2014; published 24 Jun 2014

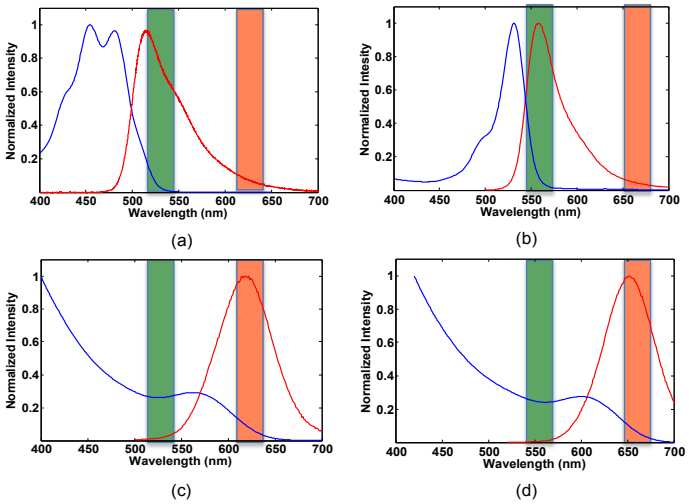

Fig. 3. Absorption (blue) and emission (red) spectra of (a) Fluorescein, (b) R6G, (c) NC 615, and (d) NC 655. The green and orange bands indicate the emission filters used for conventional imaging and NC-cp imaging, respectively.

3.2 Proximity interaction between CdTe nano-crystals and organic dye molecules

Previously we confirmed that our NCs are well anchored to the substrate so that excess rinsing by ethanol or water does not remove any of the nano-particles from the surface. Consequently, we can inject micro-droplets of fluorophores to examine the interaction between NCs and fluorophore molecules at close proximity. No ultrathin films were added between NCs and dye molecules. However, considering that there are MPA ligands connected to the NC cores that act as spacers, one can estimate that the average distances between the two is within nanometer scale.

In order to investigate the efficiency of the NC-cp technique, it is necessary that we start off with standard organic dyes (emission at λ~520 nm) that are well separated spectrally from the NC emission bands (λ~615nm). This criterion is essential for accurate detection and comparison between NC-cp and conventional fluorescence imaging method. Fluorescein and R6G are ideal samples due to their high solubility, low cost, and superior photostability. Although GFP turns out to be less photostable upon drying, we found that NC-cp imaging is capable of consistently detecting their presence at very low concentration (see Section 3.6).

For comparison purposes, it is imperative to first determine that fluorescein droplets placed on an NC thin film and imaged using a 525 nm emission filter (see Fig. 4(a)) are equivalent to conventional fluorescence microscopy acquisition as if the NC thin film were not present.

Fluorescein has peak emission at 525 nm. Since our NCs are tailored to emit maximally at 615 nm, their PL within the pass-band of the 525 nm filter is insignificant. Hence, the bright spots in Fig. 4(a) reveal directly the locations of fluorescein droplets. We have also determined that fluorescein molecules placed on top of an NC thin film experience the same excitation intensity as do the NCs. The NC thin film has coverage of approximately 75 ± 15 NC/μm^2. With absorption cross-section value of 1.27×10^{-15} cm^2 [15,16], we calculate that the effective NC thin film absorption is less than 0.1%. In addition, a separate experiment was conducted where straight-line scratches were made on the NC layer atop the glass substrate prior to micro-droplet injections (Figs. 4(a) and 4(b)). At an excitation intensity of 2.3 W/cm^2, there is no observed effect on the fluorescein PL between areas where NC is present and the scratched areas where NC is absent. This proves that the presence of NCs does not affect the PL imaging of fluorescein using the 525 nm filter. We conclude that the PL image quality of

#201235 - $15.00 USD Received 11 Apr 2014; revised 14 Jun 2014; accepted 14 Jun 2014; published 24 Jun 2014

fluorescein, viewed under the 525 nm emission filter, is equivalent to that acquired using the conventional fluorescence imaging method. Although not shown in Fig. 4, the PL of R6G and GFP are also found to be unaffected by the presence of NCs.

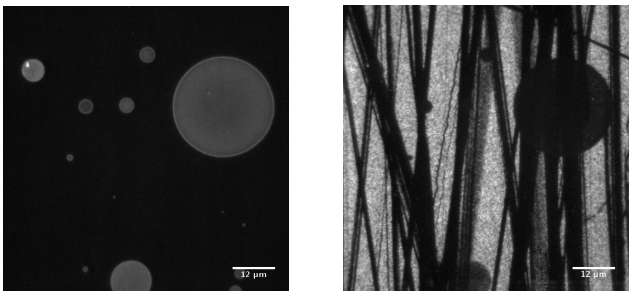

Filter 525±15 nm (a) Filter 615±15 nm (b)

Fig. 4. PL images of Fluorescein microdroplets added on top of an NC thin film, which was partially scratched using a sharp knife.(a) image acquired using a 525 ± 15 nm filter. There is no PL intensity difference between areas where NCs are present and scratched areas where NCs are absent. (b) Image acquired using a 605 ± 15 nm filter where bright areas are due to the PL from NCs, the dark straight lines are scratch marks created with the knife in order to remove the NCs, and the circular spots are regions where PL is suppressed due to NC-fluorescein close proximity interactions.

With reference to Fig. 5, the NC-cp images can be acquired from the emission filter at 615 ± 15 nm. The bright areas observed in Fig. 5(c) are the NCs PL signal at its peak value, but significant quenching is observed wherever fluorescein is present, as can be readily inferred from the dark spots in the same figure.

In order to prove that the fluorescein micro-droplets do not wash away the immobilized NCs, we proceeded to wash the sample with profuse amounts of ethanol. Eventually, the quenched NCs recovered their normal levels of PL as shown in Figs. 5(e) and 5(f). Furthermore, the fact that fluorescein can be easily rinsed away indicates that there is no strong chemical bonding between fluorescein and the NCs. This suggests that in Fig. 5(c) we are observing a close proximity, non-covalent bonding interaction. In addition, one may wonder if the observed quenching by close proximity is due to a trivial situation in which the fluorescein layer blocks the light path of the NCs toward the EMCCD. This behavior, however, is unlikely in our experiments, as our EMCCD camera is placed in the reflected path of the optical system (see Fig. 1), which means that the PL signal is being observed through the bottom of the substrate. Consequently, based on the observations in Fig. 5(c), it is clear that the PL quenching of the NCs is due to the proximity interactions.

A quantitative analysis of the NC-dye molecule interaction requires that we calculate the contrast ratio of the image. Here we define the contrast ratio as the ratio of the PL count difference (red and blue boxes in Fig. 5) with the background PL value (blue boxes).

$$\text{Contrast Ratio} = \frac{\text{PL}_{\text{red box}}^{615/525}}{\text{PL}_{\text{blue box}}^{615/525}} - 1. \qquad (1)$$

Comparative contrast ratio measurements were done between images using the two emission filters operating at λ = 525 ± 15nm and 615 ± 15 nm. The former contains peak emission of fluorescein, which is indicative of conventional fluorescence microscopy acquisition, while the latter is representative of the NC-cp imaging mode. Specifically for NC-cp acquisition, a negative contrast ratio indicates NC quenching, while a positive contrast ratio is indicative of PL enhancement. A contrast ratio of 0 would indicate no interaction between the two materials.

#201235 - $15.00 USD Received 11 Apr 2014; revised 14 Jun 2014; accepted 14 Jun 2014; published 24 Jun 2014

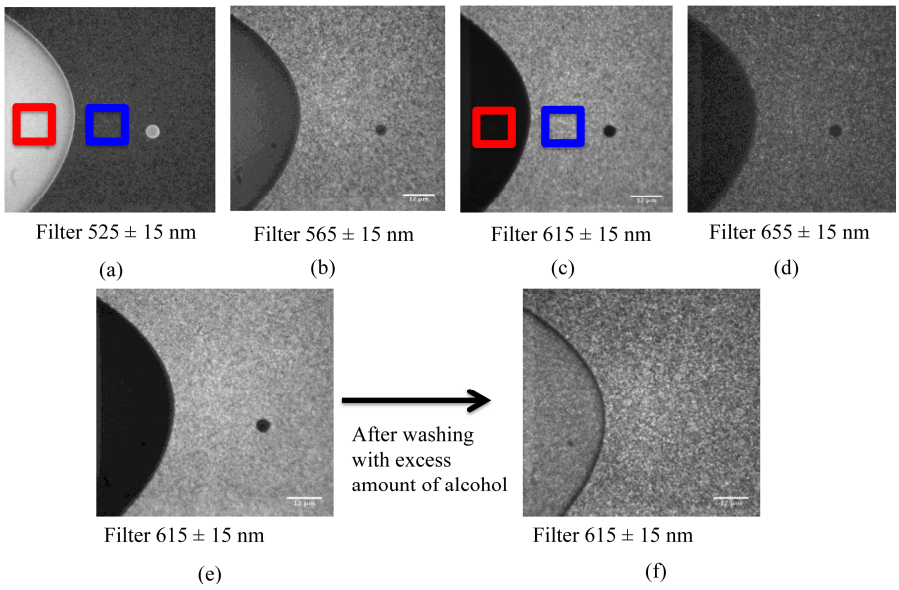

Fig. 5. (a)-(d) Photoluminescence observations of NCs (peak emission at 615 nm) immobilized on a glass substrate. Each picture is obtained through the specified bandpass filter using a wide field Zeiss fluorescence microscope. The immobilized NCs are covered with micro-droplets of fluorescein (0.0625mg/mL, peak emission at 525 nm) injected through a tapered glass needle. Injecting the solution (at a volume of <1 microL) creates a random array of droplets of different sizes. Shown in these pictures are two distinct droplets: one that has a diameter of 100 μm, and a smaller one near the center having a 5 μm diameter. It is evident from (c) that the NCs' PL is quenched wherever fluorescein molecules cover the NCs. (e) and (f) The PL of the NCs recovers after washing the sample's surface with ethanol; a residual trace of fluorescein at the droplet boundary remains visible in (f). These observations were carried out under continuous argon flow at 5 lpm to ensure a stable PL behavior of the NCs. The excitation irradiance was 2.3 W/cm^2 at 405 nm.

The fact that NCs undergo PL changes in the presence of organic dyes is not an unusual phenomenon. For example, it has been found previously that metallic nanowires sense the presence of glucose. In addition, local surface plasmon enhancement from metallic nanoparticles has been employed to sense the presence of anthrax for homeland security purposes [8,9]. However, it is found that our NCs are capable of detecting analytes with improved contrast ratio at very low concentration (~pmol of analyte per cm^2 area). Shown in Fig. 6 are the results for fluorescein and Rhodamine 6G (R6G) at different concentrations.

The magnitude of the contrast ratio with NC-cp imaging is approximately 2-3 times greater than that observed with the conventional fluorescence microscopy; see Figs. 6(a) and 6(b). Based on the contrast ratio detection limit of 0.005 on our EMCCD, we can estimate by extrapolating our data that NC-cp imaging is capable of detecting approximately 50 fluorescein/μm^2 and 100 R6G/μm^2. This is again 2-3 times lower in detection threshold compared to the conventional imaging method.

The contrast ratio obtained via conventional fluorescence microscopy increases linearly with concentration, which is the expected result. However, the NC-cp image-contrast drastically increases within the region between 500 to 2000 molecules/μm^2. This is followed by a gradual decrease beyond 2000 molecules/μm^2 for fluorescein and 5000 molecules/μm^2 for R6G. The optimal contrast ratio improvement can be found around 1000 molecules/μm^2 for fluorescein and 2000 molecules/μm^2 for R6G. The reason why the contrast ratio surpasses that of the conventional method is as yet unknown; however, one can speculate that the charge-charge interactions between analytes and NCs at close proximity entail PL quenching in a nonlinear way (more information on this in Section 3.4). At an optimal concentration of

#201235 - $15.00 USD Received 11 Apr 2014; revised 14 Jun 2014; accepted 14 Jun 2014; published 24 Jun 2014

the analyte, the magnitude of PL quenching is at a maximum. However, above such concentration, the contrast ratio decreases as evidenced in Figs. 6(c) and 6(d). A trivial explanation for this phenomenon could be simply related to the spectral leakage of the analytes. However, as shown in the orange bands in Fig. 3, the spectral overlap is a mere 8% of the total emission, which is insufficient to explain the large decrease in contrast ratio. Therefore, this leads to a more plausible explanation that PL from analytes (at λ = 525-565 nm), which falls within the absorption band of NCs (green bands in Fig. 3), could likely be absorbed and hence generates a brighter spot at λ = 615-655 nm. In order to prove that there is an additional boost in emission on the surviving NCs unaffected by the quenching effect of the analytes, we have studied carefully the change in contrast ratio as a function of irradiance at fixed analyte concentration. As expected, beyond the turning point at 2.3 W/cm^2 (see Fig. 7), NC-cp contrast ratio exhibits a very similar pattern as in Fig. 6. This proves that the remaining NCs do absorb photons from the neighboring analytes and increase in emission at a rate greater than that of the non-affected NCs.

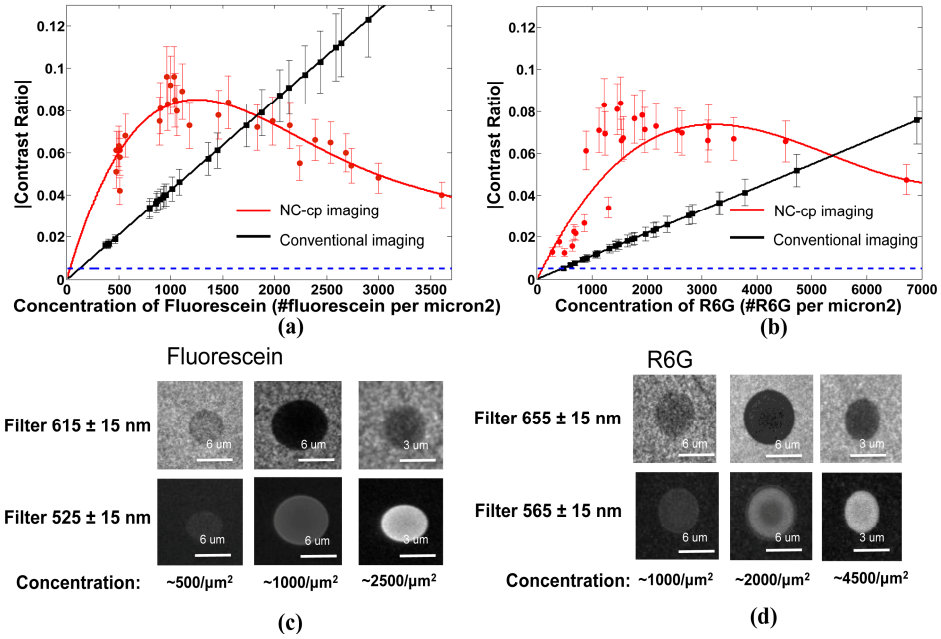

Fig. 6. Magnitude of contrast ratio comparison between NC-cp imaging and conventional fluorescence imaging. Two analytes are investigated: Fluorescein (a) and R6G (b). Concentrations of NC thin films are kept at approximately 75 ± 15 NCs/μm^2. The blue dotted line indicates the minimum detection threshold of the EMCCD (c) Actual image acquisition for fluorescein as collected by EMCCD with 615 nm and 525 nm emission filters at different concentrations. (d) Actual image acquisition for R6G as collected by EMCCD with 655 nm and 565 nm emission filters at different concentrations. Absorption cross sections for both CdTe NCs and fluorescein molecules are acquired for concentration measurements. The NC's absorption cross section is found based on the observations by Yu *et al* [14]; that of the fluorescein and R6G molecules are based on the results of Dixon and Du *et al* [15,16]. These are found to be around 1.27 × 10^{-15} cm^2 for NCs, 3.9 × 10^{-17} cm^2 for fluorescein, and 6.22 × 10^{-18}cm^2 for R6G with fixed excitation at λ = 405 nm.

#201235 - $15.00 USD Received 11 Apr 2014; revised 14 Jun 2014; accepted 14 Jun 2014; published 24 Jun 2014

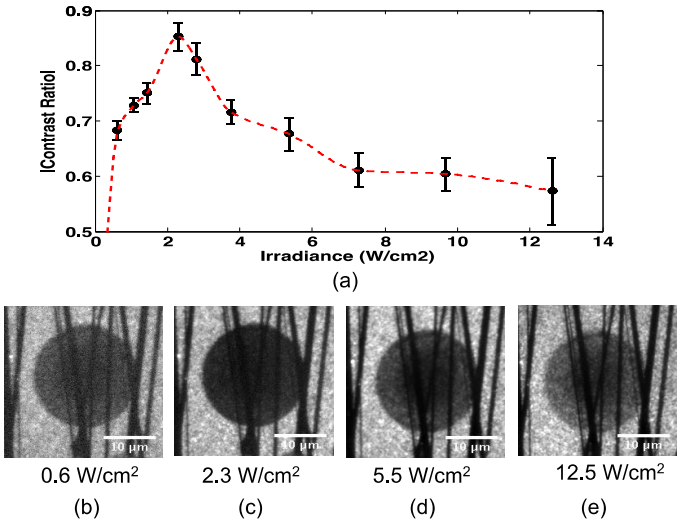

Fig. 7. (a) Magnitude of the contrast ratio as a function of irradiance of the mercury arc lamp (the illumination source) at λ = 405 nm excitation. Fluorescein micro-droplets were placed over the NC layer, as shown in frames (b)-(e), which are the actual pictures captured by the EMCCD at different irradiance levels. Deliberate scratch marks made on the NC layer are visible as straight dark lines in these pictures; this is to assess accurately the background counts as irradiance increases. The emission filter is set at 615 ± 15 nm, and the exposure time of the EMCCD is fixed at 500 ms.

3.3 Specificity of NC-cp imaging

Two types of fluorophores (R6G and Fluorescein) were added sequentially unto a uniform layer of NC 655, and both fluorophore droplets were approximately fixed at 1000 molecules/μm^2 as shown in Fig. 8(a) and 8(b). It is obvious from Fig. 8(b) that the R6G molecules are located as specified by the red circles. As we move towards the NC-cp pass-band, we can clearly see that the magnitude of the contrast ratio for R6G is lowered by a factor of two compared to that of fluorescein. This proves that NC-cp is capable of distinguishing between two fluorophores within a single pass-band. Although this is but a preliminary proof that the NCs have a higher affinity towards fluorescein, other possibilities can be realized by utilizing the NC size dependent optical properties and ligand structures [9,17] to tailor for specific molecule detection.

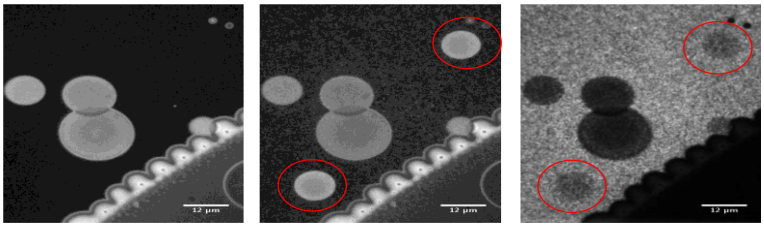

Fig. 8. (a) Fluorescein droplets viewed through the 525 ± 15 nm filter (b) Two additional droplets were found at peak emission filter of R6G (565 ± 15 nm), indicating the location of R6G droplets as depicted by the red circles. (c) Magnitude of the contrast ratio for the R6G droplets at 655 ± 15 nm filter is two times lower than that for the fluorescein droplets. This proves that NC 655 has higher sensitivity towards fluorescein at fixed concentration of 1000 molecules/μm^2.

#201235 - $15.00 USD Received 11 Apr 2014; revised 14 Jun 2014; accepted 14 Jun 2014; published 24 Jun 2014

3.4 NC-fluorescein proximity interaction at different pH levels

The exact mechanism of NC quenching in the presence of fluorescein is not fully understood. However, investigating quenching (or enhancement) of NCs under different pH conditions could provide for a better understanding of the interaction mechanism. According to Sjoback [18], at pH 4, fluorescein is in a cationic state, but as pH rises to 12, fluorescein becomes dianionic.

We conducted separate experiments with fluorescein solutions at different pH levels. Concentrations for all fluorescein solutions were normalized so that the amounts of fluorescein for all micro-droplets were kept constant, as evidenced in Fig. 9(a), which is obtained by conventional fluorescence imaging. We also ensured that basic ethanol did not create any significant PL enhancement or quenching of NCs. All of the PL values were background subtracted, and the concentration of fluorescein for all pH values were kept at approximately 1000 molecules/μm^2, which provides the maximum contrast ratio, in accordance with Fig. 6. The results of this study are shown in Fig. 9.

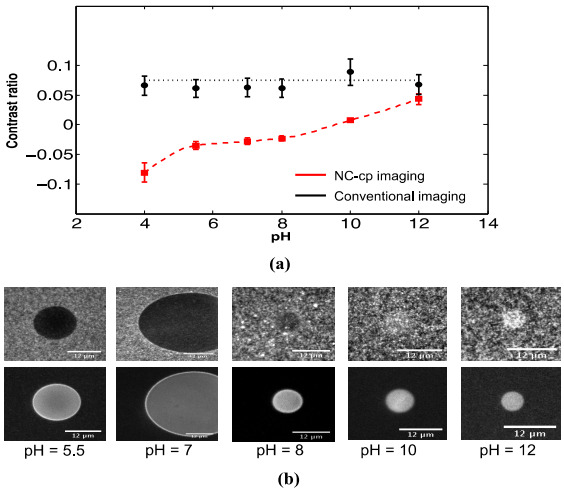

Fig. 9. (a) Contrast ratio versus the pH level of the fluorescein solution. NC-cp imaging in red, conventional imaging in black. (b) EMCCD-captured photographs showing the results of changing the pH from 5.5 to 12. The top row is obtained with the emission filter at 615 ± 15 nm, while the bottom row corresponds to the 525 ± 15 nm filter. The concentration of fluorescein at the NC layer is kept at 1000 molecules/μm^2, which provides maximum contrast, according to Fig. 6.

According to Fig. 9(a), the contrast ratio of NCs initially shows a strong quenching effect, but, as the pH increases, the contrast ratio first increases and eventually turns positive, which indicates the enhancement of the PL signal in the presence of fluorescein. Figure 9(b) (top row) shows the actual image collected by the EMCCD for the 615 ± 15 nm emission filter. We verified the presence of fluorescein in all the affected spots; see the bottom row in Fig. 9(b), which has been captured with the 525 ± 15 nm filter.

The contrast reversal of NCs as pH increases supports the hypothesis that NC PL enhancement and quenching is a result of changes in the fluorescein charge states. At pH 4, the cationic fluorescein draws the electron from the electron-hole pair generated within the NC towards the dye molecule. This impedes radiative recombination, resulting in quenching. This quenching mechanism is analogous to the photo-oxidation process. Singlet oxygen created by UV excitation reacts with the tellurium atoms on the surface of the NCs. As a result, the surface of the NC after photo-oxidation becomes a composite of $CdTe_xO_{1-x}$ with a lower bandgap than CdTe. This eventually becomes a trap site for electrons that blocks radiative recombination [13,19]. The main difference between these two situations is that

#201235 - $15.00 USD Received 11 Apr 2014; revised 14 Jun 2014; accepted 14 Jun 2014; published 24 Jun 2014

fluorescein has a temporary (reversible) effect on NCs, as evidenced in Figs. 5(e)-5(f), whereas photo-oxidation could be permanent.

In contrast to the above situation, at pH 12, fluorescein becomes dianionic. This negative charge state passivates the surface of the NCs, thereby increasing the electron-hole recombination rate. Such a mechanism for NC photoluminescence enhancement has been reported previously. In 2008, Ko *et al* [13] found that NCs become brighter when exposed to 1% agarose gel. From their observations, Ko and associates concluded that their NCs' PL has been enhanced due to the strong electronegativity of agarose gel that results in the filling of the NCs' surface trapping sites.

3.5 Long duration studies of NC-fluorescein proximity interactions

To further understand the performance of our NC particles in the presence of dye molecules, we investigated the time-line trajectory of the contrast ratio over a period of 40 minutes. This is to determine whether the NC particles could be used to sense the presence of fluorophores over long periods of time. We scattered an array of fluorescein micro-droplets over an NC-coated substrate and measured the PL of the affected regions. Small scratches were made on the NC layer atop the glass substrate in advance of micro-droplet injections in order to keep track of the real-time background intensity (see the inset in Fig. 10).

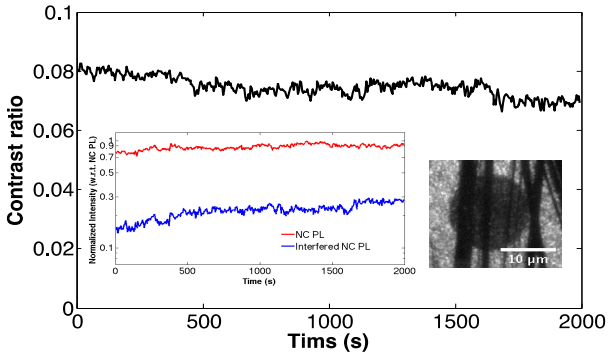

Fig. 10. Plot of the contrast ratio versus time for NC regions of a sample covered with fluorescein molecules. The inset at right shows an actual EMCCD picture of the sample, where the fluorescein micro-droplet clearly suppresses the NC PL getting through 615 ± 15nm emission filter. The scratch marks were deliberately made to measure the real time background intensity. The inset at left shows the PL signals of the NCs with and without coverage by fluorescein. Excitation irradiance was set at 2 W/cm^2 and the exposure time for each frame was 2s. The sample was exposed to continuous argon flow at 5 lpm.

Over a period of 40 minutes, the contrast ratio declines by less than 10%, as shown in Fig. 10. This indicates good reliability for long duration measurements. In order to better understand this slight reduction of the contrast ratio, the PL of both bare NC and affected NC were determined. Both of these values were subtracted from the real time background profile. From the left inset of Fig. 10, it is expected that water-soluble CdTe NCs (red curve) do not exhibit any signs of photobleaching consistent with the result found in [20]. However, the PL of affected NCs (blue curve) increases by about 15%. This indicates the photobleaching of fluorescein molecules. It is likely that, as described in section 3.2, reduction of the contrast ratio could be caused by a declining number of photo-activated fluroescein molecules. In spite of the fact that NCs do not exhibit significant photobleaching under argon flow; this is not necessarily true for the fluorescein molecules. All micro-droplets were pre-dried for 10 minutes under continuous argon flow at 5 lpm before excitation; therefore, it is unlikely that the increase in the PL of the affected region is due to the drying of the micro-droplets.

#201235 - $15.00 USD Received 11 Apr 2014; revised 14 Jun 2014; accepted 14 Jun 2014; published 24 Jun 2014

3.6 Summary

The contrast ratio comparison between the NC-cp imaging and conventional fluorescence microscopy has been summarized in Table 1:

Table 1. Measured contrast ratio for all the samples reported in this paper. Measurements were made with sample concentrations that give the highest contrast ratio. The NC thin film concentration was kept at about 150 ± 30 NCs per square micron. Excitation wavelength and intensity were fixed at 405 nm and 2.3 W/cm^2, respectively. Depending on the type of NC thin film, observations were made either at 615 nm or at 655 nm, as indicated.

Sample/Analyte	Concentration (molecules/μm^2)	Contrast ratio (NC-cp imaging)	Contrast Ratio (Conventional)	Type of Nano Crystal Affixed to Substrate
Fluorescein (pH 4)	1000 ± 200	−0.090 ± 0.010	0.066 ± 0.010	NC 615
Fluorescein (pH 5.5)	1000 ± 200	−0.035 ± 0.006	0.061 ± 0.010	NC 615
Fluorescein (pH 7)	1000 ± 200	−0.028 ± 0.004	0.062 ± 0.010	NC 615
Fluorescein (pH 8)	1000 ± 200	−0.023 ± 0.002	0.062 ± 0.010	NC 615
Fluorescein (pH 10)	1000 ± 200	0.007 ± 0.001	0.089 ± 0.010	NC 615
Fluorescein (pH 12)	1000 ± 200	0.043 ± 0.006	0.067 ± 0.010	NC 615
Fluorescein (pH 4)	1000 ± 200	−0.084 ± 0.010	0.063 ± 0.010	NC 655
R6G (pH 4)	2000 ± 250	−0.080 ± 0.010	0.021 ± 0.005	NC 655
GFP (pH 7)	115 ± 25	0.060 ± 0.010	0.022 ± 0.005	NC 615
GFP (pH 7)	115 ± 25	0.065 ± 0.010	0.022 ± 0.005	NC 655

There is little doubt that NC-cp imaging is capable of providing greater contrast ratio compared to the conventional methods. In particular, the NCs have high sensitivity towards a commercially available green fluorescent protein (Alexa Fluor 488) that absorbs and emits maximally at 495 nm and 519 nm respectively. This resulted in 3-times greater contrast ratio at ultralow concentration (115 GFP/μm^2). Shown in Fig. 11 is a comparison between images acquired via conventional fluorescence imaging and NC-cp imaging. This substantial enhancement of the contrast ratio could be due to the size of the GFP molecule, which is roughly 5-10 times greater than that of an organic dye (e.g., Fluorescein or R6G).

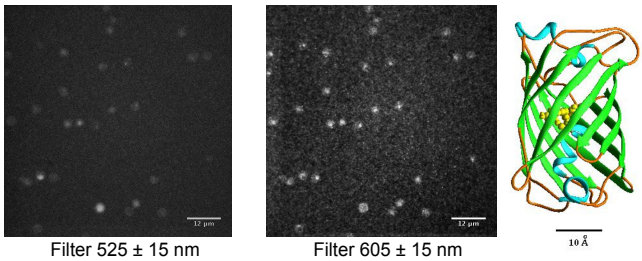

Fig. 11. Enhanced contrast ratio for the NC-cp imaging in (b) compared to the GFP microdroplets acquired via the conventional fluorescence method (a). The wild type GFP with peak emission at 515 nm has insignificant spectral leakage [22] at 615 nm pass-band. (c) The structure of GFP is a cage-like structure with a width of 1 nm and length of about 4 nm. It is approximately 5-10 times larger than the R6G and Fluorescein molecules.

#201235 - $15.00 USD Received 11 Apr 2014; revised 14 Jun 2014; accepted 14 Jun 2014; published 24 Jun 2014

3.7 Future application for super-resolution microscopy technique

Demonstrating that dried CdTe NCs immobilized on a glass substrate do in fact exhibit significant photoluminescence response towards organic dyes opens up a path toward a novel and simple approach for high-resolution optical microscopy.

Assuming that one can create a uniform or non-uniform array of NCs with approximately 50 nm spacing, each NC having a different fluorescence wavelength with good photostability, one can then easily arrange for monitoring the proximity of various nano-objects (e.g., organic or bio-molecules) to individual NCs of this array (see Fig. 12). NCs affected by proximity to (or contact with) the nano-object will experience either enhancement or quenching of their PL, depending on the charge states and the types of nano-objects under investigation. This method of microscopy can achieve sub-wavelength resolution despite the fact that its illumination and collection optics are the same conventional far-field optics used in ordinary microscopes. However, achieving sub-wavelength resolution comes at the expense of added complexity for separating the fluorescence wavelengths emitted by several NC particles affixed to different regions of the substrate. For example, if a protein molecule embedded in a phospholipid membrane atop the glass substrate is moving within a diffraction-limited pixel (~200 nm), then its exact location can be determined with the additional spectral information obtained from the NCs that are located within a diffraction-limited spot. Although finding the spectral profile of a single NC may be challenging, a practical solution would be to add a transmission grating before the CCD detector in a conventional fluorescence microscope [21]. By analyzing the change in the overall photoluminescence spectrum occurring within a diffraction-limited area of the substrate (e.g., ~200 × 200 nm^2), one can extract additional information about the location, size, shape, and nature of the molecules/objects under investigation. Unlike other microscopy techniques that rely on pulsed/patterned illumination and complex optical setups, the method proposed here simply relies on a pre-fabricated substrate covered with an array of NCs acting as nanosensors. Our method has simple illumination irradiance requirements (~2.3 W/cm^2, continuous wave at λ = 405 nm), and, aside from the need to distinguish the PL signal from different NCs, it does not require major changes to the available far field optical microscope designs.

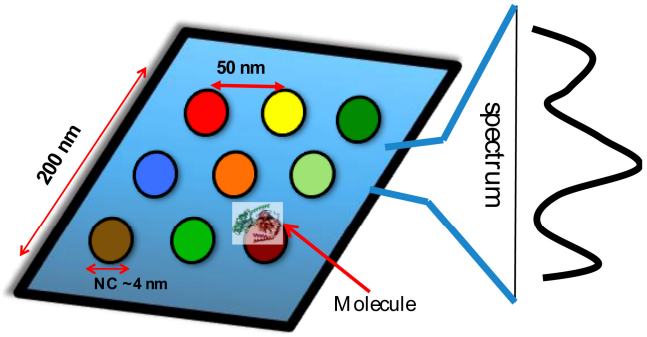

Fig. 12. Schematic view of an array of NCs with different emission wavelengths, affixed to a glass substrate and covering a typical area of 200 × 200 nm^2, with 50 nm spacing. An organic molecule coming into contact with (or in close proximity to) an NC will affect the NC's photoluminescence at the specific location, hence changing the spectral profile of the array. By monitoring the spectral changes and correlating them with the known coordinates of the various NCs, one can obtain sub-wavelength-resolution information about the movements of the organic molecule.

4. Conclusion

We have demonstrated that NCs can be used to sense the presence of fluorophores and fluorescent proteins in their proximity via a reversible quenching or enhancement of the PL of

#201235 - $15.00 USD Received 11 Apr 2014; revised 14 Jun 2014; accepted 14 Jun 2014; published 24 Jun 2014

the NC particles. The NCs PL changes were investigated as functions of the concentration of the analyte, types of analyte, pH of analyte, and duration of the excitation. These results are summarized in Table 1. It is found that the observed contrast ratio from NC-cp imaging is about 2 to 3 times greater than that obtained with conventional fluorescence imaging at an analyte concentration range of pmol/cm^2. Our imaging method is also capable of measuring the charge states of the analytes, thus providing a possible option for high throughput and high sensitivity screening for molecule detection.

Furthermore, NC-cp imaging establishes the feasibility of using the observed effects for super-resolution optical microscopy of the kind described in the preceding section. Such measurements could be further improved by investigating the corresponding spectral shifts and fluorescence lifetimes. As a result, quantifying the relevant parameters could provide a fingerprint for detection of specific analytes. Detecting non-fluorescent molecules (such as bovine serum albumin (BSA), glucose, fructose, amino acids, etc.) is still a challenge because, unlike fluorescent molecules, it is presently impossible to determine the location and concentration of these non-fluorescent species. However, attaching these molecules to a functionalized AFM tip and bringing them into the vicinity of NCs could provide a viable method of quantifying the corresponding changes in the PL of various NCs. This method is presently under investigation so as to demonstrate that our ultrastable, water-soluble, CdTe NCs can be used as molecular sensors in a wide variety of applications.

Acknowledgments

The authors gratefully acknowledge the support of the DAPRA ZOE program, the NSF CIAN ERC program under Grant No. EEC 0812072, and the Air Force Office of Scientific Research (AFOSR) BioPAINTS MURI program under Grant No. FA9550-10-1-0555.

#201235 - $15.00 USD Received 11 Apr 2014; revised 14 Jun 2014; accepted 14 Jun 2014; published 24 Jun 2014